The Determination of the In-Situ Elastic Properties of Rock Salt with a 3-Dimensional Velocity Log

Dean M. Christensen
Birdwell Division of
Seismograph Service Corp.

ABSTRACT

A 3-Dimensional Velocity Log is the commercial name used to describe an acoustic logging system capable of initiating compressional wave energy in a fluid-filled borehole and recording th travel time for longitudinal and shear waves propagating in the surrounding solid. From the recorded data the velocities of these elastic waves can be calculated, assuming the compressional disturbance at the borehole wall is a plane wave.

This type logging system has been used for nearly five years in oil reconnaissance work, and more recently, in studying the influences of nuclear explosions underground. In particular, by combining the recorded data from 3-D logs with that obtained from density logs, the physical properties of NaCl in the Tatum Salt Dome near Hattiesburg, Mississippi, have been determined.

In this paper, a description of the 3-D system is given showing how the recorded data is cor related with amplitude and frequency of a propagated wave. This is followed by an analysis of a segment of a 3-D record obtained from the Tatum survey and includes an examination of the influence of temperature, pressure, and crystal orientation to show that the calculated stiffness and compliance coefficients for the salt dome are in good agreement with data from laboratory measurements.

INTRODUCTION

As the result of interest in subsurface research, many different techniques for logging the physical properties of the earth and evaluating the reaction of rock material to artificially induced energy have been developed.

Among the several methods employed in fluid-filled drill holes today, are those which utilize acoustic energy as a source and record in numerous ways the influence of the acoustic waves whicl propagate in the surrounding solid. Some of the significant parameters which are analyzed include the absorption of energy, the crystallographic structure, the elastic properties, and strain energy of igneous and sedimentary media. Through these properties, a better understanding of the functional characteristics which motivate changes and stability of the earth's crust may be acquired.

The objective in this paper is to describe a logging system known commercially as a 3-Dimensional Velocity Log which is presently being utilized for the determination of the physical properties of NaCl in a salt dome for a nuclear test program conducted by the AEC.

Examples using data from the records obtained in the salt dome are correlated with laboratory data to show the present accuracy of 3-D to provide in-situ properties.

THE 3-DIMENSIONAL VELOCITY LOG

The 3-D Velocity Log is basically the combined system of a single-receiver down-hole continuous velocity sonde, the associated circuitry, and a recording oscillographic system located in a surface vehicle. The recorded data represents the travel time for propagation of elastic wave energy resulting from the interaction of a compressional wave incident normal and obliquely to the interface boundary of a fluid-filled drill hole.

Standard single and two-receiver CVL systems have been in use for several years and the literature describing such logging methods usually uses the two-dimensional diagram as shown in Fig. 1A. The symbols are, respectively, the diameter of the drill hole D, the distance between sonde and bore wall X (it will always be assumed the sonde is centralized), the separation between transmitter and second receiver Z, the travel path along the boundary L and L', and r_0 the path over which the compressional wave travels in the fluid.

The transmitter is a short cylinder constructed of laminated layers of material possessing magnetostrictive properties. A coil is wound around this cylinder in toroidal fashion and by introducing a pulse of current to the coil, polarizing and alternating fluxes produce displacement of the cylinder in a circumferential direction. The result is an axially dispersed disturbance which propagates radially outward as a beam of acoustic energy.

Since a beam of energy is more descriptive of the source, a ray of energy represented by the single line in Fig. 1A can only define an infinitely small fraction of the total energy. Also, according to fundamental theory, more than one angle of incidence contributes to the propagated energy. Thus, a more general diagrammatic analogy is given in Fig. 1B to indicate the extremities of three distinct "beams" defined by BB', PP', and SS'.

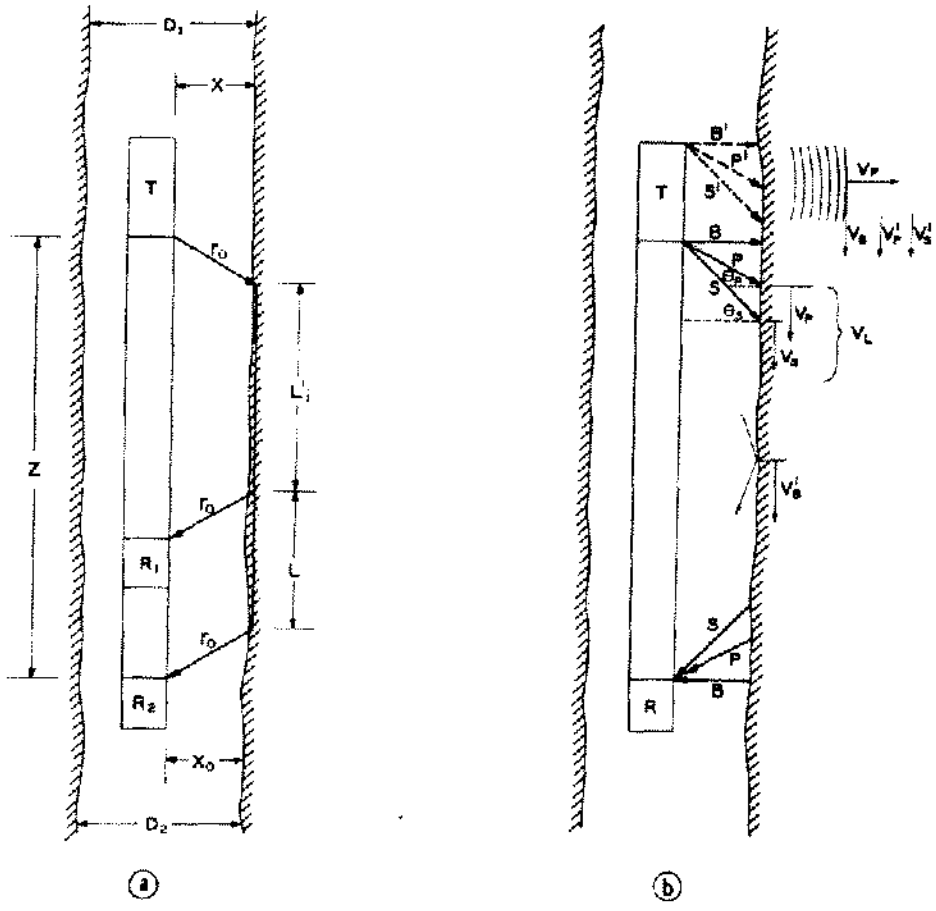

Figure 1

The important assumptions are that the interaction of the wave disturbance at the boundary can be described on the basis of approximations to geometrical optics and that the incident energy at the boundary are plane waves.

Referring to Fig. 1B, it is observed that two beams are incident at the boundary with angles ϕ_p and ϕ_s, while the third is incident normal to the boundary. In accordance with Snell's Law, if the velocity of compressional waves in the fluid is V_f and the two velocities of elastic waves in the solid are given by V_p and V_s, then

$$\text{Sin } \phi_p = V_f/V_p \quad (1)$$

and

$$\text{Sin } \phi_s = V_f/V_s \quad (2)$$

These angles represent a critical incidence where total internal reflection ensues, and the energy of a longitudinal (pressure) wave V_p and of a transverse (shear) wave V_s will propagate along the boundary. For the compressional wave incident normal to the boundary, (BB') the induced stress produces a physical displacement of the medium and the energy propagates along the boundary with a velocity V_b (such as might be seen when a tightly drawn wire is plucked). Such elastic disturbances may or may not be dispersive, and for the moment are referred to as Stonely Waves, Conical Waves, Tube Waves (Lamb Waves), or Rayleight Waves, depending upon the geometry of the well, the fluid-solid properties and a multitude of other complexities, the subject of which will not be covered in this paper. However, the interaction of the (BB') energy will also induce pressure waves and shear waves to propagate along the boundary, although their characteristics are not precisely the same as those arising at critical incidences (Christensen, 1964).

Let it be imagined that a receiver is installed within the fluid so that one ray can be displayed on an oscilloscope at the output of the receiver. This display could have a shape similar to the sine wave in the diagram (solid curve) of Fig. 2. Such phenomena is representative of a damped forced oscillation. In the limits of any one beam, an infinite number of these ray paths all parallel to one another define the flow of energy toward the solid boundary. Now, at the boundary, within the fluid, the wave fronts of all rays arrive in phase, whereas on the other side of the boundary, in the solid, they will be out of phase. As a result of the plane wave assumption, all energy within one beam add so the amplitude is greatly increased but with the addition of phase distortion resulting in a complex wave form (the dotted line of Fig. 2 with receiver at point V_p of Fig. 1B).

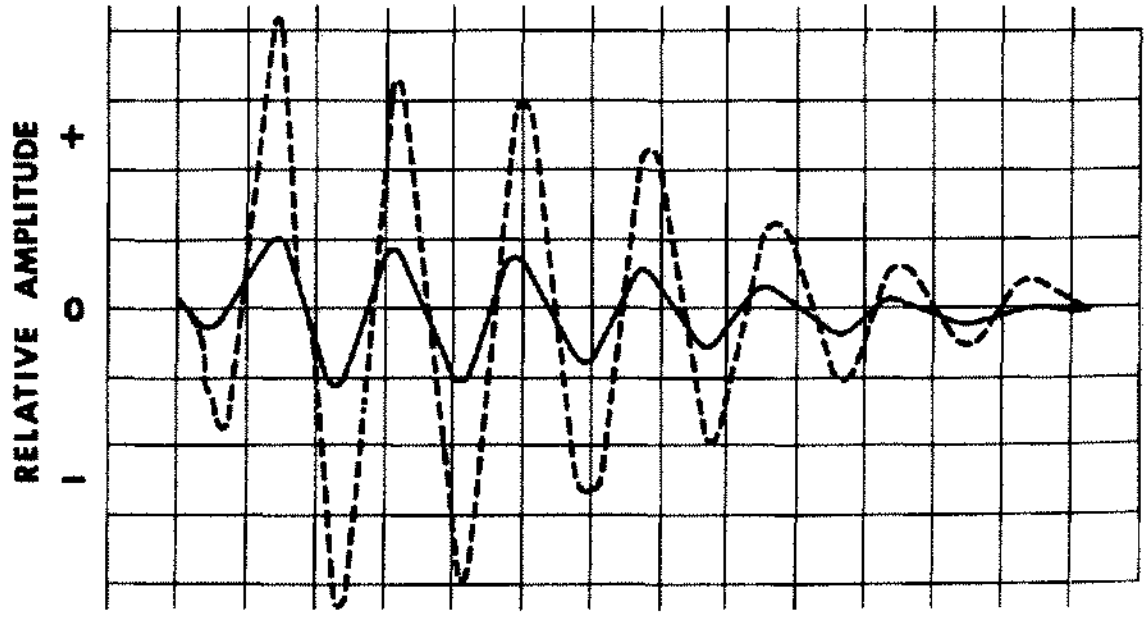

Figure 2

If the receiver is now moved to some point further along the boundary (Fig. 1B) and if each pulse to the transmitter causes the oscilloscope to sweep once, the superimposed energy from the three beams will produce the complex wave form of Fig. 3A. An example of an actual signal display observed on an oscilloscope is shown in the photograph of Fig. 3B.

Since the basic wave function is that of a damped force oscillation, the frequency of such a wave will be described by its individual parts (each beam) as a quasi-frequency; where $\omega = 2\pi f$, and $\omega_o = 2\pi f_o$

$$\omega^2 = \omega_o^2 - \gamma^2 \tag{3}$$

and f_o is the natural frequency of undamped waves and γ is a function of the attenuation and absorption characteristics of the medium. Thus, in this form of presentation, amplitude, frequency, and time of arrival are recorded.

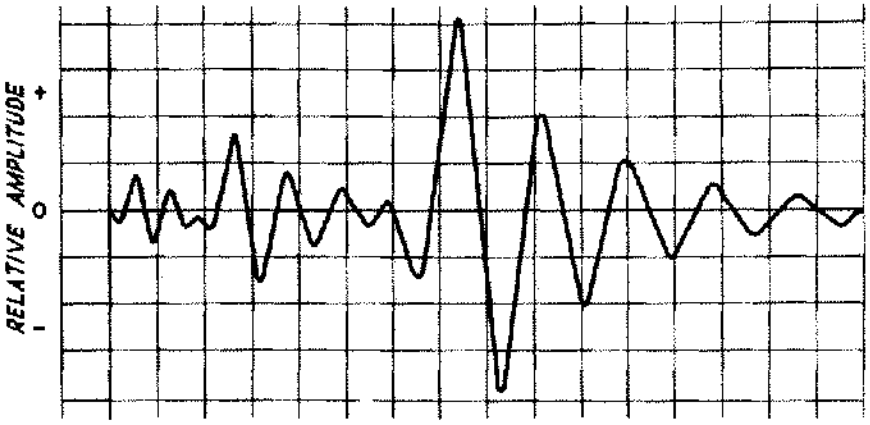

Figure 3A

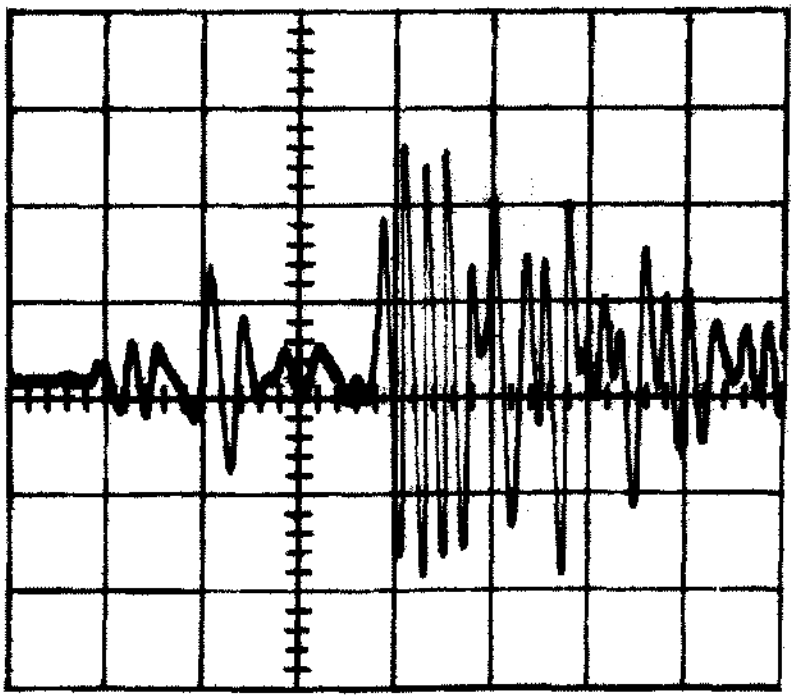

Figure 3B

If the signal of Fig. 3A or 3B is introduced into the z-axis grid of another oscilloscope, it can readily be observed that the beam will be intensified and blanked alternately as the wave amplitude varies from positive to negative. In this format of recording, frequency and arrival time are recorded, but now amplitude is reflected as a darkness or lightness of the sweep. By projecting such a sweep image onto a film which moves across the focal plane in syncronism with the motion of the sonde, a composite recording of the propagated acoustic energy is obtained. Figure 4 represents a simplified diagram of such a system. This technique was the prototype system first used commercially. In the present Fibre Optic system, the oscilloscope and projection components are totally enclosed in a vacuum tube where the focal plane is the fibre surface of the tube.

The reproduction of a typical 3-D record using the fibre optics recording system is shown in Fig. 5. The vertical scale corresponds to depth, while the horizontal scale defines travel time -- zero time on the left increasing to a maximum time on the right. The first broad dark line identified as P corresponds to the first arrival energy referred to as a pressure wave. Subsequent lines of varying width and intensity (variation in the darkness) are representative of successive energy arrivals. S and B define the point in time for arrival of the shear wave and boundary wave, respectively.

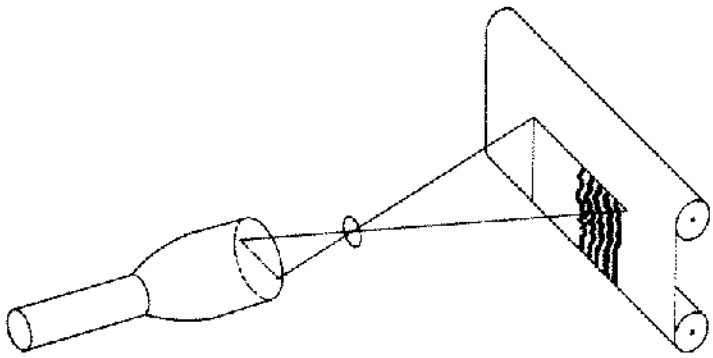

Figure 4

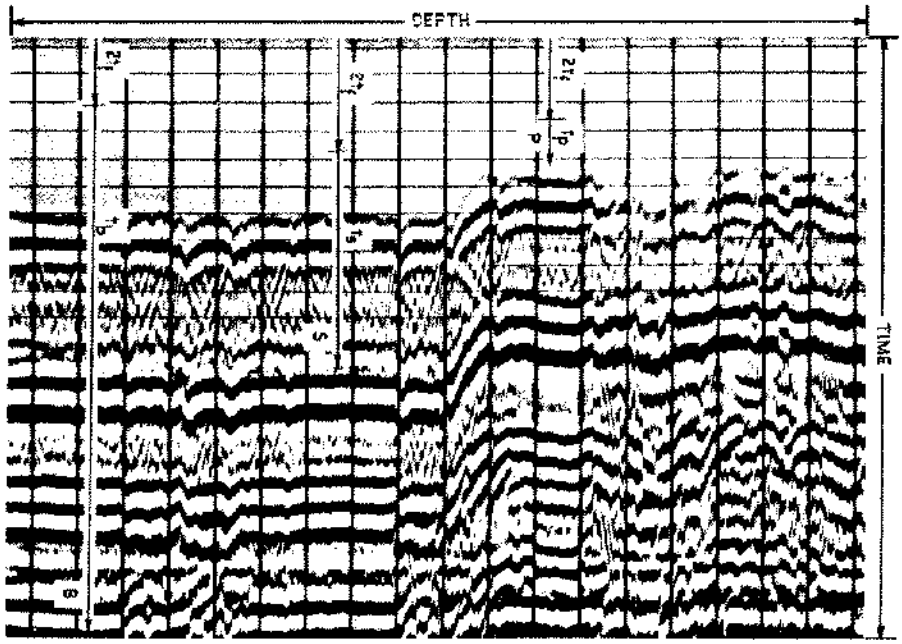

Figure 5

APPLICATION OF 3-D LOGS

Although the scheme just described was first introduced for commercial use in 1960, it was in March of 1963 that the University of California Lawrence Radiation Laboratory requested the Birdwell Division of SSC to run the 3-D log in two instrumentation wells penetrating the Tatum Salt Dome near Hattiesburg, Mississippi. Again in the late summer of 1964, three additional wells were surveyed and, more recently, during the first four months of 1965, two additional wells were surveyed.

Now, the purpose of the surveys in Mississippi was to obtain in-situ values of the elastic properties of the salt. The data is then used for defining various characteristics of the media subjected to a nuclear device.

In this particular area, a fairly thick anhydrite bed extends from about 1,000 feet to nearly 1,480 feet below ground surface, and below this level the salt extends downward. The average density of the anhydrite is about 2.90 gm/cm^3, and that of the salt is about 2.24 gm/cm. An ambient temperature recorded in the various wells ran in the neighborhood of 43°C at the depths of investigation, and an overburden stress calculated to be around 200 bars.

Core samples were obtained from the Dome indicating that the major portion of NaCl exists in a conglomerate mass of small crystals having an average cubic edge dimension of about 2 cm. However, in discreet zones near the top of the salt, large crystals with cubic edges at least four inches or larger were obtained. A comparison of such crystals with a small segment of conglomerate salt are displayed in the photograph of Fig. 6A. In Fig. 6B, the inclination of the large crystal shows that one plain has a preferred orientation of about 15 to 20 degrees.

Referring now to the section of 3-D log in Fig. 5, the first arrival pressure wave and shear wave have been noted. The first timing line is 600 microseconds from zero with subsequent timing lines at 100 microsecond intervals. The frequencies and velocities reflected by the time of arrival for this depth interval are such that the wave length for the pressure wave and shear wave are approximately λ_p = 21 cm and λ_s = 11 cm, respectively. Thus, for the conglomerate mass of salt, these wave lengths are large compared to crystal size.

Calculation of the two velocities is determined on the basis of an empirical equation discussed in an early paper (Christensen, 1964) and given here as

$$V\beta = [Z - 2F\ (d)\ \mathrm{Tan}\{\mathrm{Sin}^{-1}\ \tau\beta/\tau_f\}]/T\beta \qquad (4)$$

where Z is the separation between transducers, τ_f the fluid travel time over Z, $\tau\beta$ the recorded time (β refers to P wave or S wave), $T\beta$ the difference between recorded time and mud time, and F (d) a constant which is a function of the borehole diameter and sonde length.

As a benefit of recording both P waves and S waves, assuming the media were isotropic and logging the density of the salt, permits the usual isotropic moduli to be calculated from the following equation:

$$B = \rho\,(V_p^2 - 4/3\ V_s^2) \qquad (5)$$

$$E = 3B(1 - 2\delta_o) \qquad (6)$$

$$\mu = \rho\, V_s^2 \qquad (7)$$

$$\sigma_o = [1/2\ (V_p/V_s)^2 - 1]/[(V_p/V_s)^2 - 1] \qquad (8)$$

where the four terms are commonly referred to as the bulk compression modulus B, Young's modulus E, the Shear modulus μ and Poisson's ratio σ_o.

In the depth interval discussed above, the pertinent properties obtained through equations 5 through 8 are given in Table I.

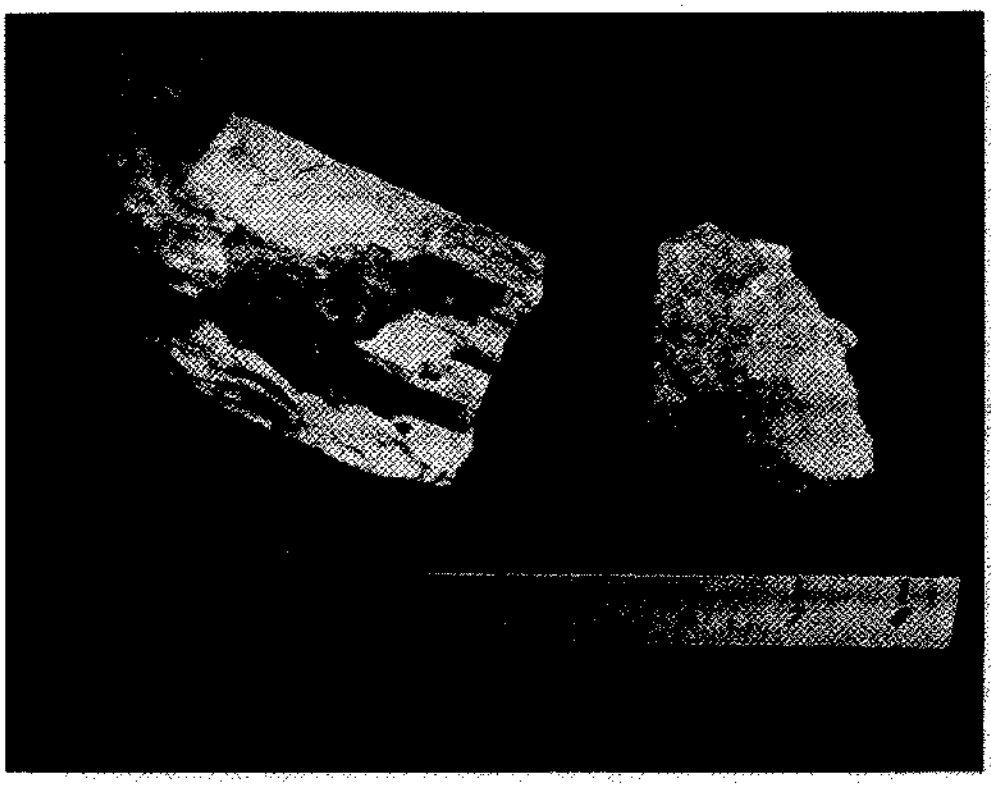

Figure 6A

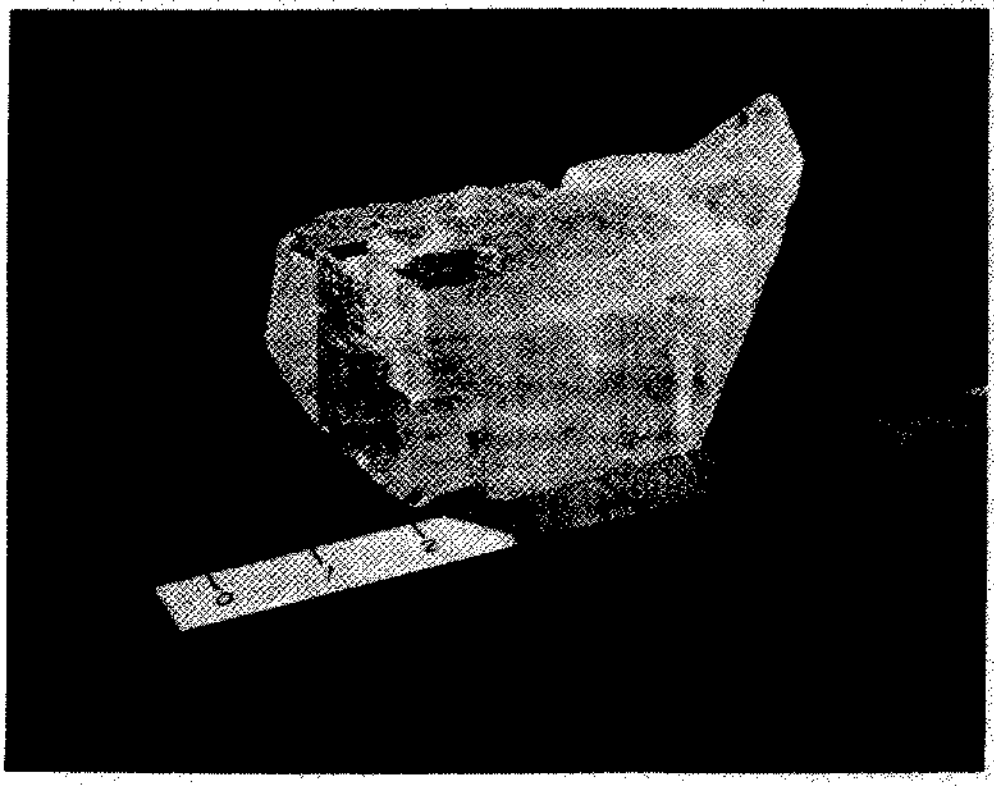

Figure 6B

TABLE I: ISOTROPIC ELASTIC MODULI

V_p	V_s	σ_o	μ	B	E	ρ
Meters/Sec.			Units $\times 10^{11}$		dynes/cm^2	gm/cm^3
4665	2445	0.310	1.34	3.07	3.51	2.24

Several questions may be raised at this point, mainly, those concerned with the accuracy of the data when certain broad assumptions have been used.

The first may be that which assumes elastic isotropy when obviously salt is anisotropic. A partial answer is found in the fact that polycrystalline conglomerate solids are usually elastically isotropic or nearly so because the individual anisotropy of randomly oriented grains cancel, and an average elastic constant is obtained. On the other hand, if a preferred orientation of such solids exist, the deviation from some known value will be reflected by the method of calculation of these moduli which depend on the degree of anisotropy.

In reference to known values for the elastic constants of NaCl, numerous laboratory studies have been conducted over the past 40 years. Many of these studies have included the influences on the numerical values when the crystals have been subject to a range of pressures and temperatures. Still others have studied the variation in the value of each moduli as a function of crystal orientation.

To examine these characteristics, it is most often preferable to use a set of terms known simply as the Coefficients of Compliance S_{ij}, and stiffness C_{ij}, as used in the following equation relating stress and strain (Mason, 1958).

$$\Delta_i = S_{ij}\ T_j \tag{9}$$

$$T_i = C_{ij}\ \Delta_j \tag{10}$$

where Δ_i and T_i are the strain and stress, respectively. The relationship between the four elastic moduli given above and the compliance coefficients is given by:

$$E_j = \frac{1}{S_{ij}}\ (i = j < 3) \tag{11}$$

$$\mu k1 = \frac{1}{S_{k1}}\ (k = 1 > 3) \tag{12}$$

$$\sigma_{ij} = \frac{-S_{ij}}{E_j}\ (i \neq j < 3) \tag{13}$$

$$B = \frac{1}{3}\ (S_{11} + 2\,S_{12}) \tag{14}$$

noting that B is independent of the choice of axis.

Without dealing with the complexities of Tensor Calculus, it suffices to note that the elastic behavior of a completely asymmetric body is specified by 21 independent coefficients. For cubic structures this number reduces to 3, and because the property surface of a homogeneous isotropic medium is a sphere, the number reduces to 2.

A complete set of coefficient terms for NaCl reported by numerous references is given in Table II. The average value of these terms and a comparison with calculated coefficients for the in-situ measurements are given, where $C_{11} = \rho V_p^2$ and assuming $C_{44} = C_{12} = \rho V_s^2$ is also included.

The data given in Table II, obtained from laboratory measurements are unique in that a priori temperature, pressure, and orientation were established as room temperature, pressure, and the stresses applied with reference to principal axis (i.e., zero rotation of axis).

TABLE II: COEFFICIENTS OF COMPLIANCE AND STIFFNESS

REFERENCE	S_{11}	S_{12}	S_{44}	C_{11}	C_{12}	C_{44}
	units $\times 10^{-13}$ cm/dyne			units $\times 10^{11}$ dynes/cm		
Bridgemann	23.0	-5.00	78.0	4.70	1.23	1.28
Durand	22.5	-4.67	78.7	4.99	1.31	1.26
Hunter	22.8	-4.50	78.1	4.86	1.19	1.28
Lazarus	22.7	-4.50	78.1	4.91	1.23	1.28
Huntington	24.9	-4.60	78.7	4.85	1.23	1.26
Bergman	24.1	-5.00	84.0	4.67	1.23	1.19
Galt	22.9	-4.60	78.7	4.87	1.24	1.26
Average	23.3	-4.70	79.2	4.84	1.24	1.26
In-Situ	23.3	-5.01	74.6	4.87	1.34	1.34
Error	0%	6%	6%	0.6%	7%	6%

In order to provide a more realistic comparison between laboratory data and that obtained from 3-D logs, it suffices to normalize the laboratory data as a function of these three parameters.

The influence of temperature on the stiffness coefficient is given by Bond (1943), as:

$$C_{ij}^{*} = C_{ij}(1 + tT_{ij}^{*}) \tag{15}$$

where T_{ij}^{*} is the temperature coefficient of the stiffness function; with t the temperature of the crystal. Bond (1939), Hunter (1941), and Rose (1935) have determined the C_{ij} variation over a range of temperature from $0°K < t < 1000°K$. Graphically the influence is given in the diagram of Fig. 7.

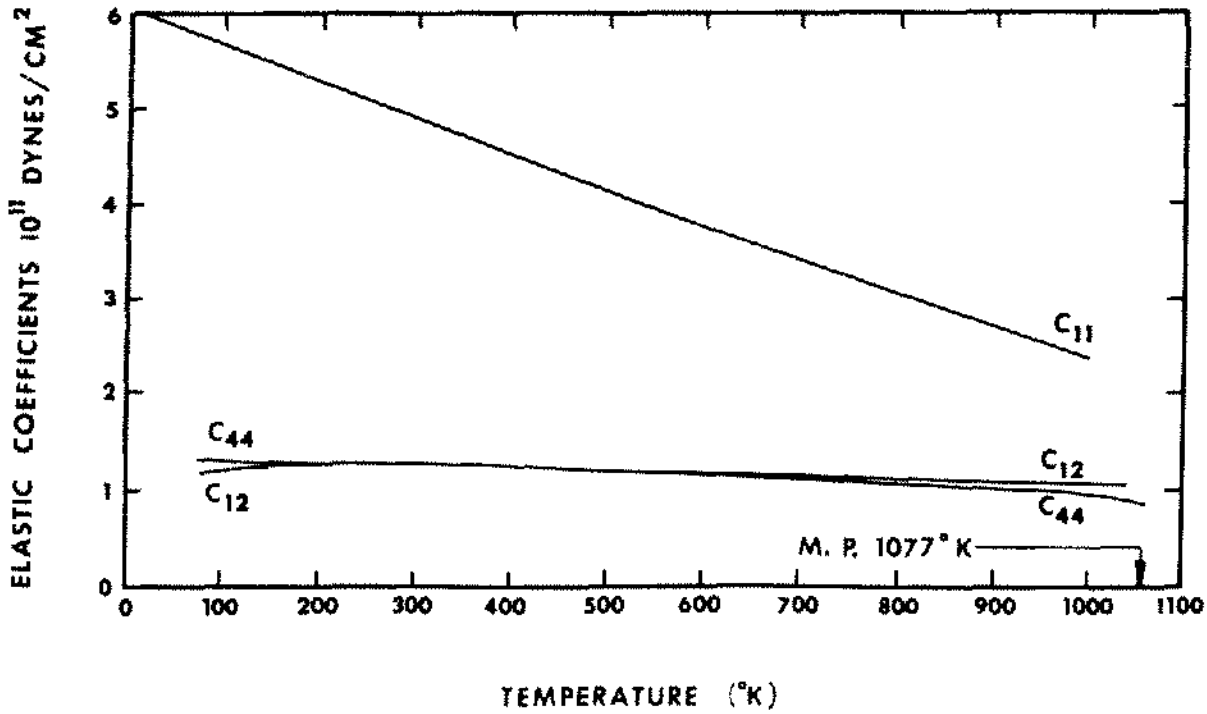

Figure 7

The influence of pressure on the stiffness coefficients has been studied by Lazarus (1949) and Decker (1965) from which the graph of Fig. 8 is obtained.

For increase in temperature C_{11} is a decreasing function, while C_{12} and C_{44} are essentially uninfluenced. For increase pressure all three coefficients increase in magnitude.

The variation of C_{ij} and S_{ij} for cubic structures as a function of rotation of principal axis have been studied by Bond (1943), Hearmon (1946), and Wortman (1965). From these references, the notation for orientation can be written as:

$$C'_{11} = C_{11} + C_n [(L_X)^4 + (M_X)^4 + (N_X)^4 - 1] \quad (16)$$

$$C'_{12} = C_{12} + C_n [(L_X L_Y)^2 + (M_X M_Y)^2 + (N_X N_Y)^2] \quad (17)$$

$$C'_{44} = C_{44} + C_n [(L_Y L_Z)^2 + (M_Y M_Z)^2 + (N_Y N_Z)^2] \quad (18)$$

where $C_n = (C_{11} - C_{12} - 2C_{44})$ and L, M, N, are the direction cosines.

Taking the values of temperature = 43°C, pressure = 200 bars (1 bar $\cong$ 1 atmosphere), and preferred orientation about 15 degrees, the normalized coefficients will not have the value given in Table III.

TABLE III: NORMALIZED COEFFICIENTS FOR LABORATORY DATA

REFERENCE	S_{11}	S_{12}	S_{44}	C_{11}	C_{12}	C_{44}
	Units $\times 10^{-13}$		cm^2/dyne	Units $\times 10^{11}$		dyne/cm^2
Laboratory	24.2	-5.28	76.3	4.20	1.31	1.32
In-Situ	23.3	-5.01	74.6	4.87	1.34	1.34
Error	4%	5%	2%	4%	2%	2%

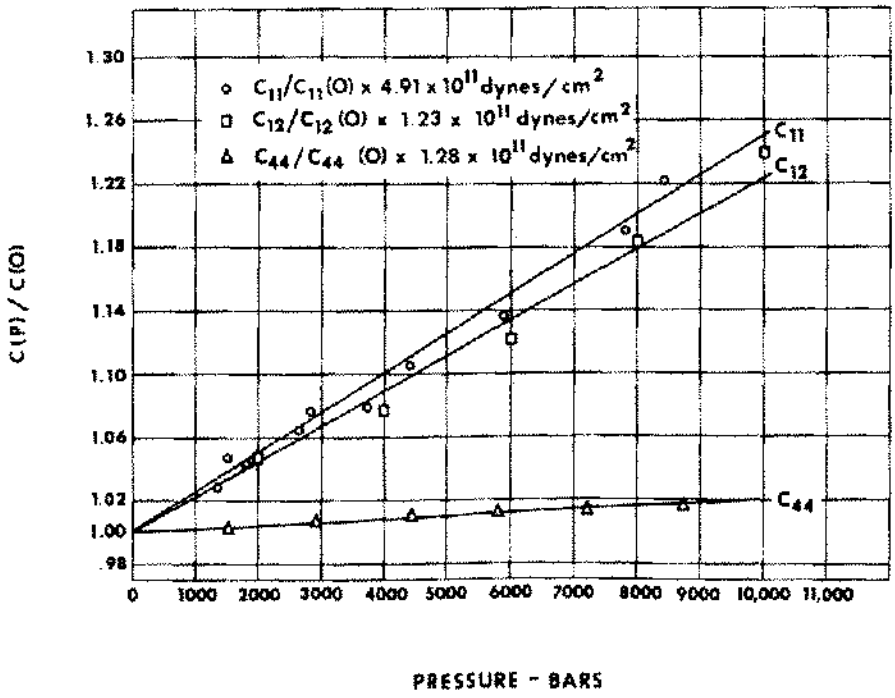

Figure 8

As is the case in this paper, it is the elastic moduli which are being sought after. Taking the data of Table III and using equations 11 through 14, the Anisotropic Elastic Moduli are given in Table IV for comparison with the data from Table I.

TABLE IV: ANISOTROPIC ELASTIC MODULI

REFERENCE	σ	μ	B	E
		Units $\times 10^{11}$		dynes/cm^2
Lab: Anisotropic	0.219	1.32	2.45	4.13
In-Situ Anisotropic	0.215	1.34	2.56	4.29
In-Situ Isotropic	0.310	1.34	3.07	3.51

Comparison of data from Table IV shows a significant difference between anisotropic and isotropic values as would be expected. The measurements performed in-situ assume isotropy because the wave length is large compared to a crystal size. To calculate these properties for comparison purposes requires that the elastic properties be independent of direction and that the body remain in equilibrium under a shearing stress. Because the properties given in Table IV are anisotropic, there must be a relationship between these and the method for calculating isotropic moduli. Such a relationship is found in the determination of the degree of anisotropy which is a function of the two deformation modes involving shear distortion of the crystals.

Note the ratio σ_o between two velocity terms as measured, and the stiffness coefficient is given by:

$$\sigma_o = C_{12}^+/2(C_{11}^+ - C_{44}^+) = C_{12}/2\,\Gamma(C_{11} - C_{44}) = \sigma/\Gamma \tag{19}$$

where

$$\Gamma = 2C_{44}/(C_{11} - C_{12}) = 0.7 \tag{20}$$

for salt. Thus, we have in terms of Lame's parameters

$$C_{12}^+ = \lambda' \qquad C_{44}^+ = \mu \qquad \text{and,} \tag{21}$$

$$C_{11}^+ = \lambda' + 2\mu \tag{22}$$

From which

$$\lambda' = 2\mu\,\sigma_o/(1 - 2\sigma_o) \qquad B = E/3(1 - 2\sigma_o) \qquad E = 2\mu(1 + \sigma_o) \text{ etc.} \tag{23}$$

and using the anisotropic values from Table IV we obtain a set of rationalized isotropic terms given in Table V, where the isotropic values from Table I are added for comparison purposes.

TABLE V: RATIONALIZED ISOTROPIC ELASTIC MODULI

REFERENCE	σ_o	μ	B	E	λ'
Laboratory (Rationalized)	0.313	1.32	3.09	3.47	2.21
In-Situ (Rationalized)	0.307	1.34	3.02	3.50	2.13
In-Situ (Isotropic)	0.310	1.34	3.07	3.51	2.19

CONCLUSIONS

To determine either coefficients of stiffness, compliance, or moduli of elasticity requires three functions: Pressure wave, Shear wave, and Density. Comparison between laboratory data and in-situ required one assumption, that Cauchy's relation $C_{12} = C_{44}$ is valid for cubic symmetry (which is true for salt but not for other crystal media). Then this comparison shows that 3-D is capable of recording the two wave velocities within an accuracy of 5% indicating the assumption concerning plane waves at the boundary is a sufficient condition. Further, that the emperical relation used for determining the velocities from raw time must also be sufficient.

The terminology used in Table IV (i.e., anisotropic; isotropic) refers to the particular equation used for calculating the moduli. Thus, on the basis of Table IV and Table V, and Γ ; so long as the wave length of the acoustic energy is large compared with crystal size, equations 5 through 8 are sufficiently proper for determining the in-situ elastic properties of salt.

REFERENCES

Bergmann, L., Ultrasonics; John Wiley, 1944.

Bond, W.L., "The Mathematics of the Physical Properties of Crystals"; Bell System Technical Journal, vol. 22, January, 1943.

Bridgemann, P.W., "The Elastic Moduli of Five Alkali Halites"; Proc. Am. Acad., vol. 64, 1929.

Christensen, D.M., "A Theoretical Analysis of Wave Propagation in Fluid Filled Drill Holes for the Interpretation of the 3-Dimensional Velocity Log"; SPWLA Fifth Annual Logging Symposium Transaction, May 13-15, 1964, Midland, Texas.

Decker, D.L., "Equation of State of NaCl and Its Use as a Pressure Gauge in High Pressure Research"; Journal of App. Phys., vol. 36, January, 1964.

Durand, M., "Temperature Variation of the Elastic Moduli of NaCl, KCl and MgO"; Phys. Rev., vol. 50, 1936.

Galt, J.K., "Mechanical Properties of NaCl, KBR, KCl"; Phy. Rev., vol. 73, June, 1948.

Hearmon, R.F.S., "The Elastic Constants of Anisotropic Material, Rev. of Mod. Phys., vol. 18, July, 1946.

Hunter, L., et al.; "The Variation with Temperature of the Principal Elastic Moduli of NaCl near the Melting Point"; Physical Rev., vol. 61, January, 1942.

Huntington, H.B., "Ultrasonic Measurements on Single Crystals"; Phy. Rev., vol. 72, August, 1947.

Lazarus, D., "The Variation of the Adiabatic Elastic Constants of KCL, NaCl, CoZn, Cu and Al with Pressure to 10,000 Bars"; Physical Rev., vol. 76, August, 1949.

Mason, W.P., Physical Acoustics and the Properties of Solids; D. Van Nostrand Co., 1958.

Rose, F.C., "The Variation of the Adiabatic Elastic Moduli of Rock Salt with Temperature Between 80°K and 270°K"; Phy. Rev., vol. 49, January, 1936.

Wortman, J., et al.; "Young's Modulus, Shear Modulus and Poisson's Ratio in Silicon and Germanium"; Jour. of App. Phys., vol. 36, January, 1965.